



Numerical investigation on Stress Intensity Factor and J Integral in Friction Stir Welded Joint through XFEM method

Imane Elmeguenni, Mohamed Mazari

Laboratory of Materials and Reactive Systems LMSR, University Djillali, Liabes, Sidi Bel-Abbes, Algeria.
imaneelmeguenni@gmail.com, mazari_m@yahoo.fr

ABSTRACT. In fracture mechanics (domain of cracked environments), it is concerned to forecast the behavior of the structures until their ruin.

Friction Stir Welding (FSW) is a new process for solid-state joining, it can weld high strength aluminum alloys from the 2000 series.

However, despite the research work carried out on the FSW process, the performance and knowledge of the mechanical strength of these welded joints remains limited. At this stage, a local analysis of each zone constituting a welded joint 2024T351 by FSW is carried out. We resort to the numerical simulation of the crack propagation in this joint is used in order to extend the mechanical integrity of this joint with a view to the numerical determination of the crack parameters that are the integral J and the stress intensity factor in each area of joint, in the presence of plasticity under the assumption of proportional loading.

We insist on the coherent cohesive zone model in the frame of the XFEM extended finite element method.

The numerical results showed that the evaluation of the global two-parameter approach to fracture mechanics in an FSW-welded structure makes it possible to evaluate the impact of the process on the failure of these FSW zones.

KEYWORDS. Friction stir welding; X-fem; Crack propagation; Stress intensity factor; J integral.



Citation: Elmeguenni, I., Mazari, M, Numerical Investigation on Stress Intensity Factor and J Integral in Friction Stir Welded Joint through XFEM method, Frattura ed Integrità Strutturale, 47 (2019) 54-64.

Received: 08.10.2018

Accepted: 19.11.2018

Published: 01.01.2019

Copyright: © 2019 This is an open access article under the terms of the CC-BY 4.0, which permits unrestricted use, distribution, and reproduction in any medium, provided the original author and source are credited.

INTRODUCTION

The FSW process was invented, developed and patented by W. Thomas in the United Kingdom in 1991. This new welding technology is in full development phase, although already applied industrially for some fabrications, in particular in aeronautics, shipbuilding and railways [1].

The principle of the FSW is to mix and plasticize the material through the heat provided by the friction between the tool and the parts to be welded. These are held rigidly to eliminate any movement during mixing, the welding is carried out in the solid state ("pasty" state) [2].

The major advantage of this process is to weld materials without reaching their melting temperature. It thus makes it possible to assemble alloys deemed difficult to weld by traditional welding processes such as aluminum, copper and titanium alloys [5].

It is agreed that the friction stir welding is not symmetrical with respect to the line of junction. This is due to the relative speed of the material relative to the tool. This results in two parts: "the advancing side (AS)" for which the speed of advance and the tangential speed of rotation of the tool are of the same direction and the "retreating side (RS)" for which the speed of advance and the tangential speed of rotation of the tool are in the opposite direction [7].

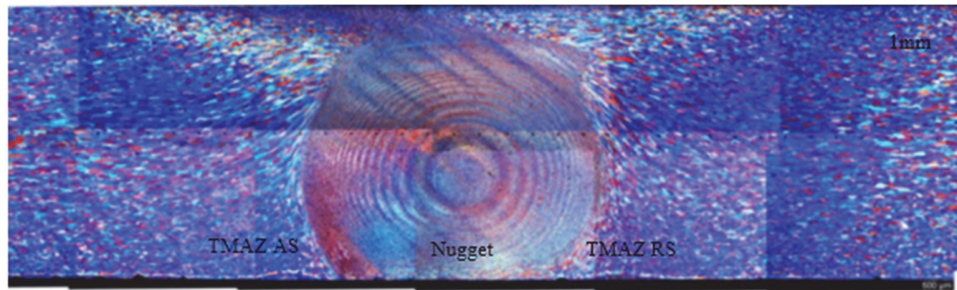


Figure 1: Mapping of a 2024 T351 welded joint after anodic attack. Optical microscopy [4].

FSW welding has a very heterogeneous microstructure along the joint. The shape of the bead, the grain size and the size of the areas constituting the joint depend heavily on the parameters of the FSW welding process, the shape of the tool as well as the heat treatment of the welded materials.

The analysis of the microstructure in terms of size and orientation of the grains makes it possible to distinguish different zones along the welded joint by FSW (Base Material (MB) - Heat Affected Zone (HAZ) - Thermo-Mechanically Affected Zone (TMAZ) and Nugget (N)).

Indeed, the thermal and mechanical load gradients experienced by welded materials involve a microstructure gradient across the weld. Note also the appearance of microstructure gradients between the AS side and the RS side of the welded joint by the FSW process [3].

FSW welding is the result of the flow of softened metal around the tool and forging through the shoulder. In general, the plasticized material on the incoming side of the seal moves around the pin to fill the void left behind the tool while passing through the outgoing side of the joint [8].

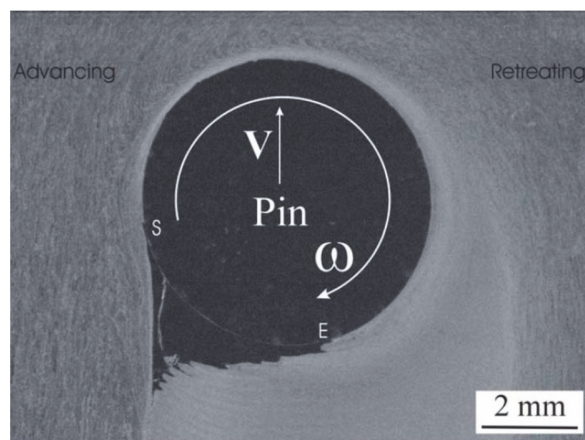


Figure 2: Deposition of material on the back of the tool [6].

The heating of the material is necessary so that an integrated joint can be manufactured. This heating lowers the flow stress of the material, which is easier to deform.

Under these conditions, the material can be moved more easily by the tool. Potential sources of heat are the plastic deformation of the material as well as the friction at the interface between the work piece and the tool. The plastic deformation of the material is a volume source of heat, while the friction generates a surface flux located at the interface piece / tool [6].



In order to simulate the phenomenon of crack propagation in a friction stir welded joint, it is then necessary to take into account the plasticity at the crack tip.

Basics of non-linear fracture mechanics

The field of application of elasto-plastic fracture mechanics is relatively broad since it ranges from small plasticity around the crack tip to ductile failure, in which the material can withstand large plastic deformations before breaking.

In the case of ductile failure, the plastic zone is no longer negligible and can extend well beyond the crack tip, we then talk about EPFM conditions (Elastic Plastic Fracture Mechanics) [9].

Plasticity can be treated as nonlinear elasticity, provided that the loading is monotonous and proportional without discharge. The nonlinear elastic material is described by the deformation energy [11].

$$W = \int_0^{\varepsilon} \sigma_{ij} d\varepsilon_{ij} \quad \sigma_{ij} = \frac{\partial w}{\partial \varepsilon_{ij}}$$

where w is the density of deformation energy.

The integral J it is no longer equal to the rate of restitution of energy G , which does not take into account the plasticity:

$$J = -\frac{dp}{da} \neq G$$

where P represents the potential energy.

The Stress and strain fields near the crack tip in elastoplastic media were connected to J by Hutchinson and Rice and Rosengren, defining the HRR fields characterizing the intensity of the stresses and deformations [10].

In order to take into account any propagation of crack, it is interesting to determine in addition to the integral J , the factors of stress intensities. These factors do not make sense if we consider the case of ductile failure, since they are defined from the elastic singularity that is difficult to identify with an extended plasticity, therefore, in the context of the EPFM assumptions, the plastic zone is always around the crack tip, but it is no longer negligible on a macroscopic scale, surrounded by a dominance zone of linear elastic asymptotic fields. This K -dominance zone allows us to continue to define the stress intensities factors as Irwin did, the elastic displacement field in this zone being rebalanced by taking into account the plasticity near the crack tip. We then define stress intensity factors that we could call elastoplastic [9].

The K -dominance zone: the size of the zone of dominance of the elastic asymptotic fields.

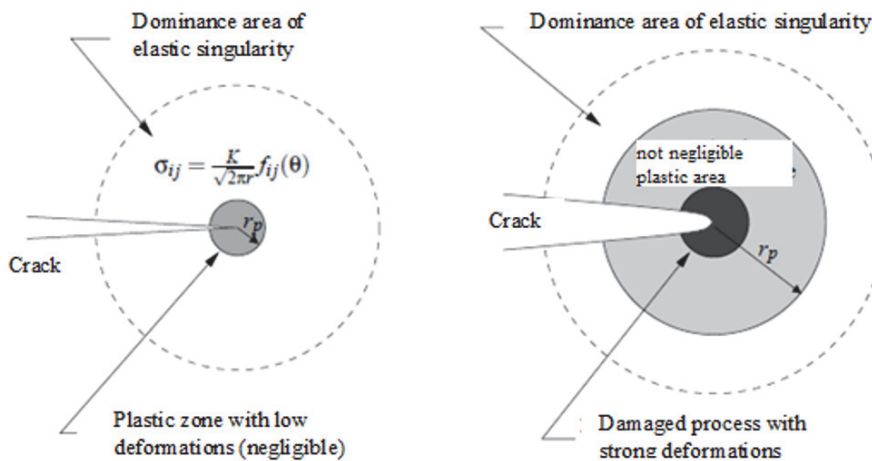


Figure 3: Dominance zones in elasticity and plasticity [9].

Numerical approach and chosen model

In order to successfully simulate crack propagation under monotonic loading we chose to use a Cohesive Zone Model (MZC) originally proposed by Dugdale (description of the plasticity near the crack tip (perfect plasticity) and by Barenblatt (Traction Law vs Opening for the decohesion of atomic networks) in the 1960s [13]. The cohesive zone models, by the

simple concepts that they introduce, like the energy of separation, can allow a simplified representation of the active zone at the crack tip and to clarify the mechanisms at the origin of the appearance and propagation of cracks [13, 10].

Cohesive models are appealing in their simplicity and the possibility that they offer to model the entire process of failure, from the initiation of a defect to the propagation of a crack. By relying on a predetermined form of cohesive law [10]. With the improvement of numerical modeling tools, this concept has become a crack propagation model that is widely used in finite element calculations because of its simplicity and its various possibilities of use [13].

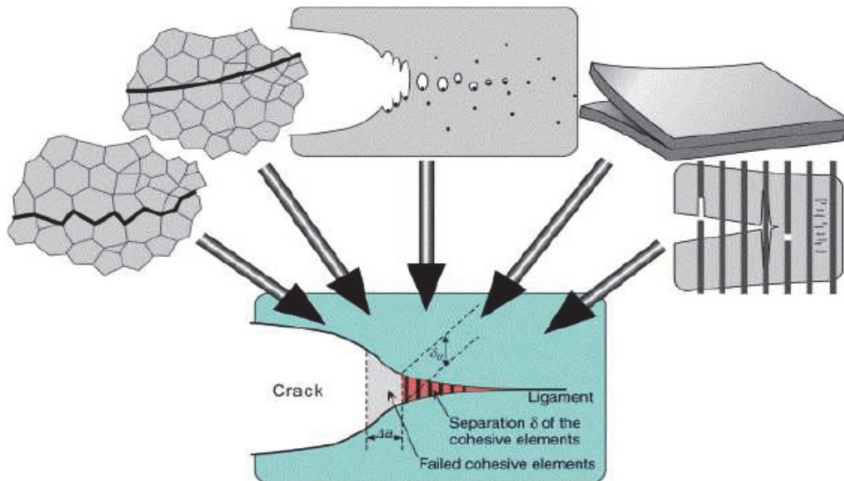


Figure 4: Schematization of crack propagation using cohesive elements [13].

The separation and the breaking of the material are controlled by a cohesive law of general shape $\sigma = f(\delta)$. The cohesive stress σ has three components: σI the normal stress, σII and σIII two tangential constraints. The cohesive elements separate when the damage appears and lose their rigidity at failure [10].

From a numerical point of view, the primary advantage that has led to the use of cohesive zone models is that their use eliminates the mesh size dependence observed with continuous mechanical models. Indeed, the area under the curve of the law of traction-separation corresponds to the work of separation of the lips of the crack per unit of area [13].

Moreover, the prediction of crack propagation modeled using cohesive zones does not require calculation of a criterion during the calculation, it arises only from the response of the cohesive zone to the loading and thus from the law of behavior that has been attributed to it [13].

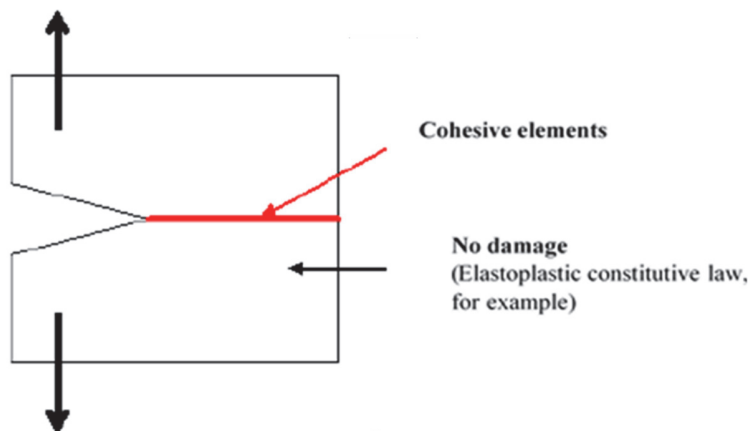


Figure 5: schematic illustration of the placement of the cohesive elements on the crack path, the damage is localized in the cohesive elements, and the behavior of the material is reacted by a continuous law of behavior [13].

However, the apparent ease of use of this method (MZC) by the association with a numerical method which knows an important development in recent years: X-FEM. Admittedly, X-FEM is not a numerical model in the true sense of the term [12], but XFEM provides a natural framework for cohesive zone models.



It allows the introduction of a mobile discontinuity, during the calculation and independently of the mesh of the studied structure. For its application to ductile failure, an extension to geometric nonlinear problems and materials has been implemented.

The extended finite elements method (X-FEM) is an extension of the MEF. This method was introduced in 1999 [MOe 99] following industrial needs to simulate the propagation of cracks in three dimensions to predict the behavior of parts in service. It has the main advantages of the MEF and it is not necessary to take into account the cracks during the meshing of the structure. It allows to introduce the presence of a defect (a crack for example) without explicitly meshing it. Only the mesh of the structure is necessary. The method is therefore very adapted to problems with mobile discontinuities because it avoids the problems of remeshing and projection during the propagation of crack. This method preserves intact the possibility of modeling complex three-dimensional structures and integrating nonlinear behavioral laws [14]. In order to integrate the presence of the crack, the enrichment function of Heaviside H is used for the nodes (Ncut) elements crossed by the crack. The element containing the crack tip is then enriched using specific asymptotic functions (Nfront nodes) [16].

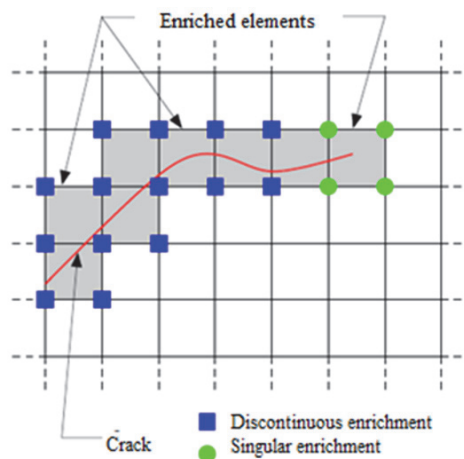


Figure 6: Any crack laced on a mesh-Enrichment strategy-[9].

Or:

Nfront is the set of nodes whose support contains the crack front.

Ncut is the set of nodes whose support is completely sliced by the crack.

The enrichments are thus made exclusively at the nodes, and their good distribution depends on the precise knowledge of the position of the crack, knowing that the latter can evolve.

The enrichment of the displacement field is made locally depending on the position of the element with respect to the plane and the crack front, that is, according to the values of the level functions [15].

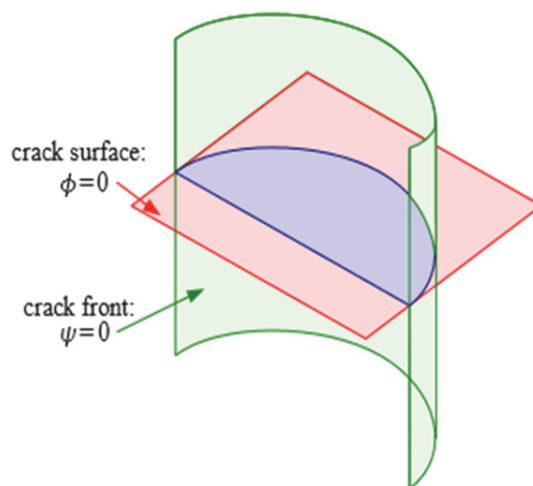


Figure 7: Defining the geometry of the crack from the pair of level functions [15].

When the crack slices an element, the integration support of the element changes. In the case of non-linear materials, the variables are time dependent and the projections of fields can introduce errors difficult to control. Stress concentrations are usually localized at the point of the crack. This is why an area located in a radius R_{pla} , centered on the crack tip is over-integrated in the same way as the sliced elements, in order to anticipate the arrival of the crack. This method was proposed by Elguedj and Prabel for non-linear materials. It can be considered as a local refining to describe more precisely the fields at the crack tip [17].

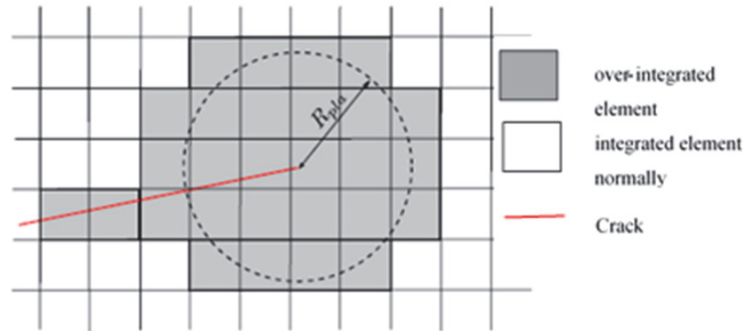


Figure 8: Taking into account the plasticity at the crack point [17].

FSW regimes	NZ	TMAZ	HAZ	PZ
Young's modulus (GPa)	68	68	68	68
Poisson's ratio	0.33	0.33	0.33	0.33
Yield stress (MPa)	350	272	448	370
Hardening constant	-	800	719	770
Hardening exponent	-	0.1266	0.05546	0.086
Hardness (Hv1)				
Residual stress (MPa)	142 -41	118 95	167 -20	132 0

Table 1: Material properties of FSW zones [18].

PZ		HAZ		TMAZ		NZ	
Strain	Stress	Strain	Stress	Strain	Stress	Strain	Stress
0.0003	20	0.0004	25	0.0007	50.34	0.00044	30.43
0.0006	40	0.0006	35	0.00123	75.86	0.0008	51.30
0.0009	45	0.0010	58	0.0016	106.9	0.0012	69.56
0.0014	90	0.00126	83	0.0020	131.03	0.0015	91.30
0.0021	125	0.0015	95	0.0031	186.21	0.0021	130.43
0.0034	220	0.0020	130	0.0045	268.96	0.0032	186.95
0.0050	300	0.0028	175	0.0057	331.03	0.0043	286.96
0.0058	320	0.00438	280			0.0055	331.91
0.0084	440	0.00558	330				
0.0120	487	0.00898	480				
		0.01166	540				

Table 2: Stress-strain data of FSW zones [18].

NUMERICAL MODELING OF CRACK PROPAGATION IN AN FSW JOINT ON THE MATERIAL 2024T351

To better understand the concepts of the global approach in fracture mechanics in a welded joint by the FSW welding process we simulate the phenomenon of crack propagation under static loading in mode I in the different zones of the joint on an alloy of the series 2000 (with structural hardening), namely the 2024 T351 in which the thermal history, the deformation and the precipitation evolve in a coupled way [4].



Alloy 2024 T351 is used for the lightening of transport structures. However, this alloy is difficult to weld conventionally. The microstructure and the mechanical behavior of FSW welds of this alloy have been finely characterized and detailed by C. Genevois et al [4] (Fig. 1).

To model numerically crack propagation we chose a rectangular thin plate pre-cracked ($a_0 = 3\text{mm}$) dimensions $60 \times 20 \times 1$. The mechanical properties of the different zones were determined from metallographic observations of the joint [18].

Then we developed a FSW welded joint in 3D using the calculation code by EF ABAQUS.

The properties of the alloy 2024-T351 in the different zones of the welded joint are summarized in Tabs. 1 and 2.

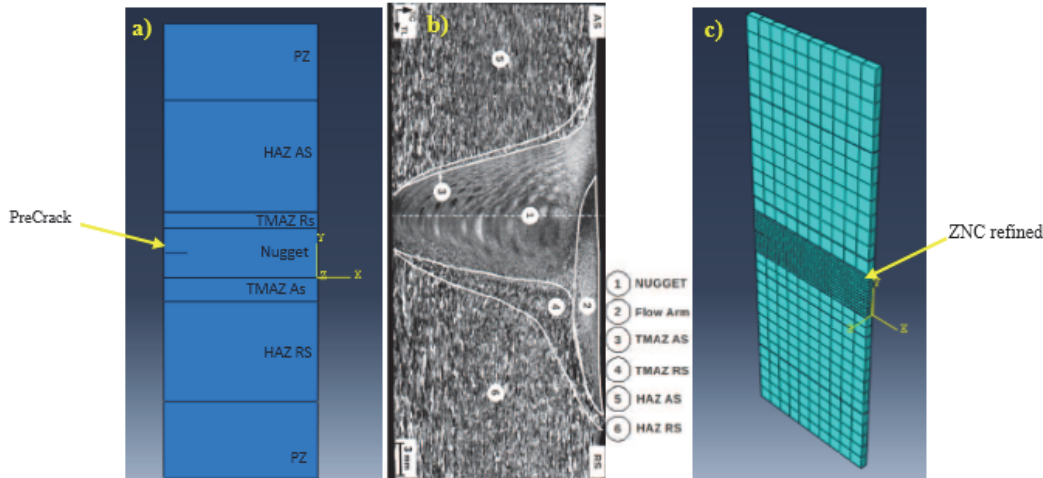


Figure 9: a) Geometry of the analyzed structure; b) Definition of the zones constituting the joint 2024T351 [3]; c) Mesh of joint 2024T351 (refined cohesive zone).

The simulation of crack propagation allowing the use of the cohesive zone method and associated by the law of evolution of the damage (initiation and propagation of crack). A variable D characterizing the damage and the effective nominal constraints and an effective displacement δ_m are introduced.

Elasto-plastic crack-tip behavior must be written in order to take into account plasticity-induced loading history effects. In the same way the mesh of the structure, elements C3D8R, that is, three-dimensional 8-node hexahedron elements with integration reduction in ABAQUS are used. By meshing finely the cracked zone, the results are much more accurate if the mesh of the cohesive zone is finer.

The contact created between the surfaces of the different zones is of type "Tie". However, it should be noted that Level Sets are updated each time the crack propagates.

The nonlinear static problem is solved by an incremental procedure coupled to an iterative solver of the Newton-Raphson type.

RESULTS AND DISCUSSIONS

In order to evaluate the integrity of the FSW-welded 2024T351 joint and its ability, and after simulating the temporal evolution of the crack propagation in each of the zones of the joint, the parameters of cracking are determined that are the integral J and the stress intensity factors of each zone.

Fig. 10 shows the simultaneous evolution of crack propagation in the different zones of the FSW joint.

Figs. 11 and 12 show the evolution of J as a function of the advance of the crack in each of the zones, the results obtained show a steady growth of J . This growth accelerates after the priming of the crack. In addition, there is a significant dispersion on the tenacities at the priming: the values range from 0.5954 in the ZAT "RS" to 2.400 J/mm² (in the BM). This dispersion may be due to variations in the properties of the ZAT, ZATM and the nugget and dissymmetry of the FSW joint.

For the priming of the base metal BM, a significant value of J of 2.400 J /mm² is noted. This value is high compared to the priming value of the ZAT RS = 0.5954 J /mm².

The results also show that the values of J at priming are low in the ZAT Rs, the ZATM AS, the ZATM RS followed by the ZAT AS.

We are also seeing that the gap of the integer J between the BM and the ZATM RS for priming is practically double. Same gap is noticed between the nugget and the ZATM RS. This leads us to conclude that the priming of the crack differs when the microstructure changes.

As a result, the evolution of J is affected by the mechanical characteristics of the ZAT, the ZATM and the nugget.

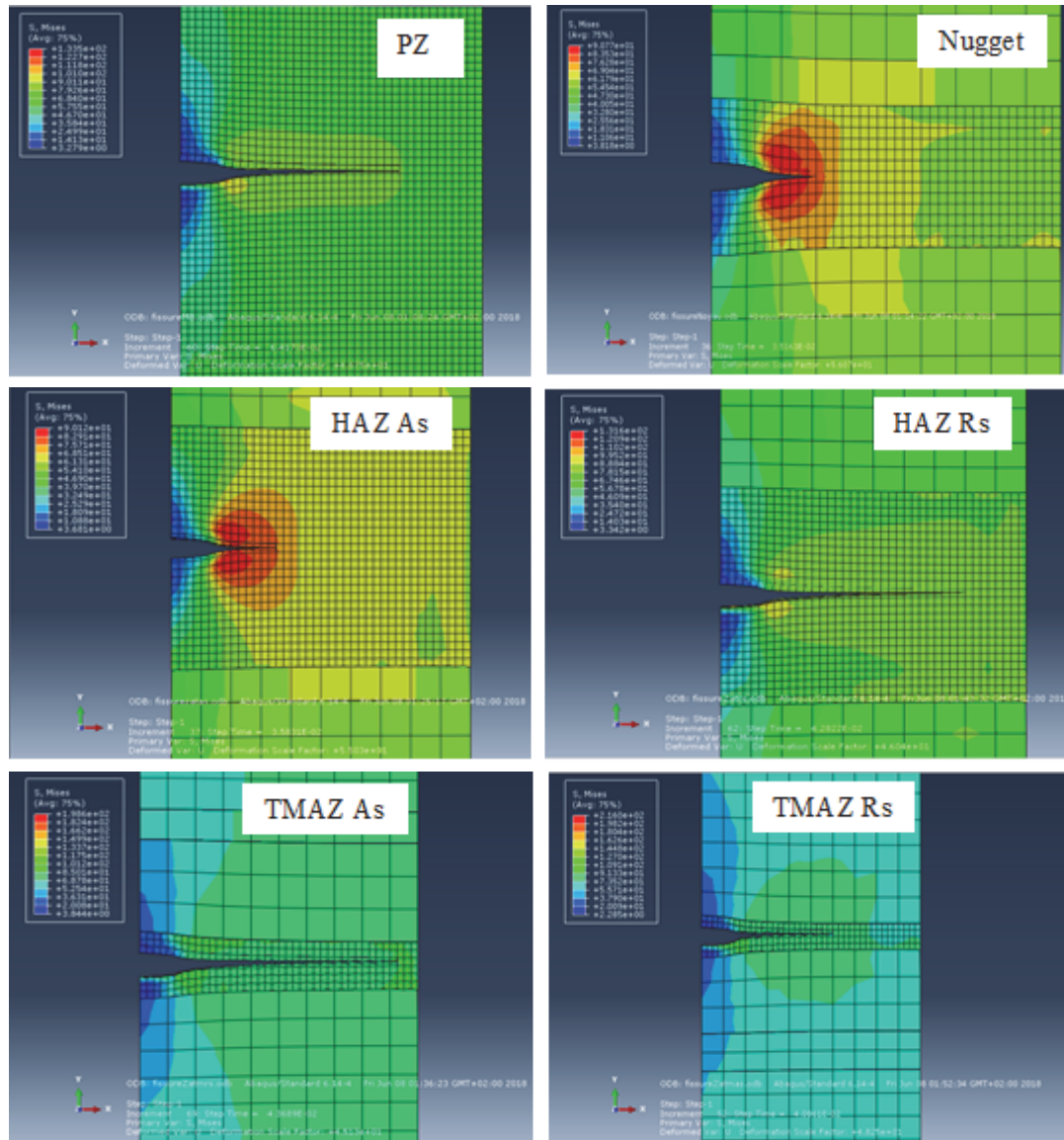


Figure 10: Crack propagation in the different zones of the FSW 2024T351 joint.

Figs. 13 and 14 represent the variation of the stress intensity factor (SIF) during the crack advance for the different zones of the welded joint by the FSW process of alloy 2024 T351. It is found that the stress intensity factor increases with the length of the crack. The asymptotic behavior is visible for all zones.

The nugget exhibits high values of the stress intensity factor relative to other areas. K_I at failure is 3.5×10^4 MPa $\sqrt{\text{mm}}$, on the other hand for the BM is $K_I = 3.2 \times 10^4$ MPa $\sqrt{\text{mm}}$. This increase is explained by the existence of additional stiffness induced by FSW welding. This leads us to note that the nugget is the most resistant zone in the FSW joint of alloy 2024T351. Through the analysis of the results, it can be seen that the lowest SIF values are for the ZAT at AS and RS where K_I at failure is equal to 2.45×10^3 MPa $\sqrt{\text{mm}}$ on the AS side and 2.5×10^3 MPa $\sqrt{\text{mm}}$ on the RS side.

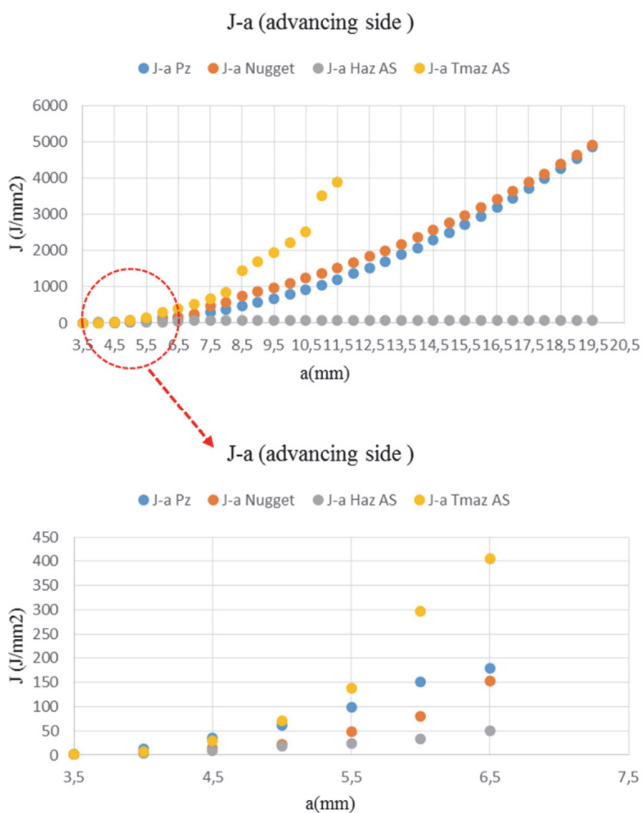


Figure 11: Evolution of the J according to the crack advance of the AS side.

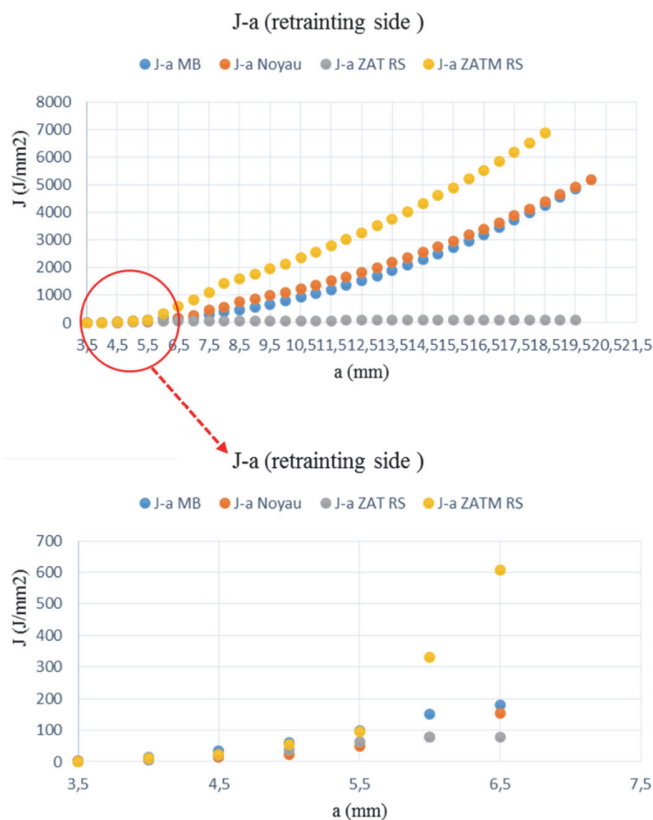


Figure 12: Evolution of the J according to the crack advance of the RS side.

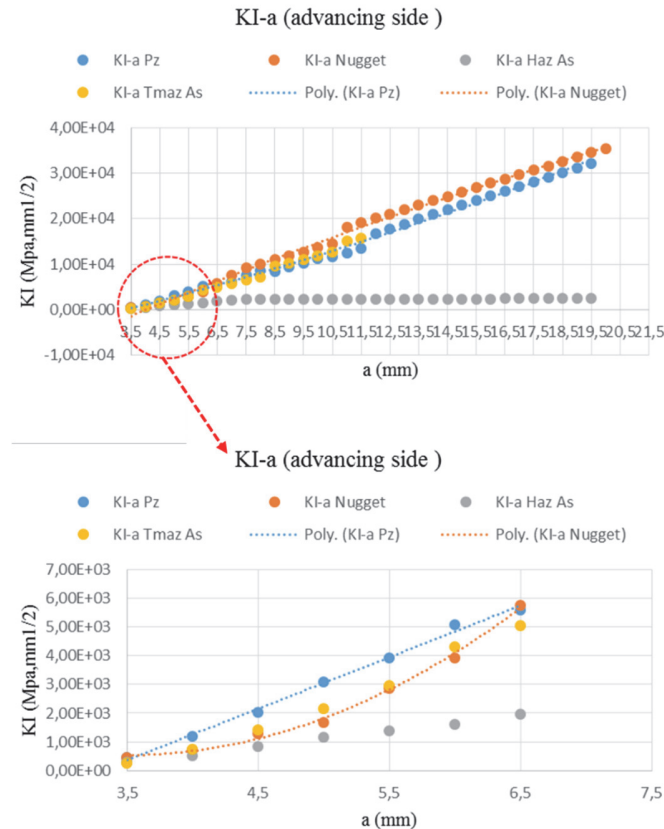


Figure 13: Variation of the SIF according to the crack advance on the AS side.

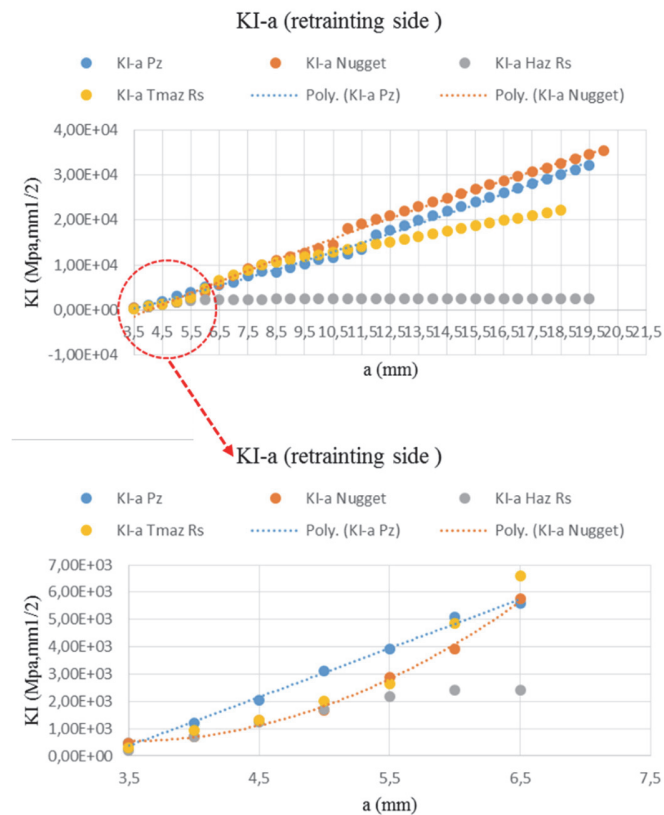


Figure 14: Variation of the SIF according to the crack advance on the RS side.



CONCLUSION

The Simulation of crack propagation, the approach adopted by binding the cohesive zone model to the extended finite element method allowed us to highlight the evolution of J and the SIF along the different areas of the welded joint by FSW.

The Priming in the different FSW zones is mainly piloted by the microstructure, and depends on the orientation of the crack with respect to the joint, whether on the AS or RS side.

The important variation of the values of J is associated with the mechanical characteristics of the different zones as well as the heterogeneities of the FSW joint.

Moreover, the growth of the SIF in the nugget leads to the evolution of their resistance, this shows the preponderant effect of the FSW welding process on the 2024 T351 alloy, indeed it governs the overall behavior of the joint.

REFERENCES

- [1] Aissani, M. (2013). Study of the thermal and mechanical behavior of aeronautical materials by numerical methods: application to the welding of metal structures, Ph. Thesis, University Saad Dahlab of Blida. Algeria.
- [2] Jemal, N. (2011). Contribution to the thermal and mechanical characterization of the welded zone in FSW, Ph.D. Thesis, National School of Arts and Crafts. (Mechanical engineering. Arts and Metiers ParisTech).
- [3] Demmouche, Y. (2012). Study of the fatigue behavior of FSW welded joints for aeronautical applications, Ph.D. Thesis, National School of Arts and Crafts.
- [4] Genevois, C. (2004). Genesis of microstructures during friction stir welding of aluminium alloy of the series 2000 & 5000 and resulting mechanical behavior, Ph.D. Thesis, Polytechnic national institute of Grenoble.
- [5] Zimmer, S., Da Costa, B., Stassart, X., Langlois, L. (2007) Friction Stir welding, Presentation of the process, Instructional Manual, Metz.
- [6] Gemme, F. (2011). Numerical modeling of the physical phenomenon of friction stir welding and fatigue behavior of 7075-t6 aluminum welded joints. Ph.D. Thesis, University of Montreal.
- [7] Guedoïri, A. (2012). A contribution to the modeling and numerical simulation of friction stir welding, Ph.D. Thesis, Arts and Metiers ParisTech. Center of Metz.
- [8] Farah, A. (2013). Fatigue behavior of joints alloy 7075-t6 welded by friction stir welding and finalized. Ph.D. Thesis, Polytechnic School of Montreal.
- [9] Elguedj, T. (2006). Numerical simulation of fatigue crack propagation by the extended finite element method: taken into account plasticity and friction contact, Ph.D. Thesis, National Institute of Applied Sciences of Lyon.
- [10] Simatos, A. (2010). X-fem method for the modeling of large propagation of crack in ductile tear. Ph.D. Thesis, National Institute of Applied Sciences of Lyon.
- [11] Al Rassis, A. (1995). Contribution to the study of hot ductile tear in welded joints and numerical modeling in global approach and local approach, Ph.D. Thesis, University of Science and Technology of Lille.
- [12] Hamon, F. (2010). Modeling of the mechanical behavior in cracking of aeronautical alloys. Ph.D. Thesis, National school of Mechanics and Aerotechnics-Politiers.
- [13] Moriconi, C. (2012). Model of fatigue crack propagation assisted by hydrogen gas in metallics, Ph.D. Thesis, National school of Mechanics and Aerotechnics-Politiers.
- [14] Trollé, B. (2014). Multi-scale simulation of fatigue crack propagation in rails. Ph.D. Thesis, National Institute of Applied Sciences of Lyon.
- [15] Prabel, B. (2007). Modeling with the x-fem method of dynamic propagation and cleavage crack arrest in a rep. Ph.D. Thesis, National Institute of Applied Sciences of Lyon.
- [16] Dartois, S. (2009) Extension of a multiscale cracking model in mixed mode and implementation in X-FEM code. 19th French congress of Mechanics. Marseille.
- [17] Pelée, R. (2014). Extension of the X-FEM approach in fast dynamics for three-dimensional crack propagation in ductile materials, Ph.D. Thesis, National Institute of Applied Sciences of Lyon.
- [18] Andrijana, D., Danijila, Z., Aleksandar, G., Aleksandar, S., Marko, R., Horia, D., Snezana, K., (2015). Numerical simulation of crack propagation in friction stir welded joint made of Al 2024T351 alloy, Int. J. of Engineering Failure Analysis, 58, pp. 477-484.